

Heat and Momentum Transport of Ion Internal Transport Barrier Plasmas on Large Helical Device

K. Nagaoka, K. Ida, M. Yoshinuma, Y. Takeiri, M. Yokoyama, S. Morita, K. Tanaka, T. Ido, A. Shimizu, N. Tamura, H. Funaba, S. Murakami¹⁾, K. Ikeda, M. Osakabe, K. Tsumori, H. Nakano, O. Kaneko and LHD experiment group

National Institute for Fusion Science, Toki 509-5292, Japan

1) Department of Nuclear Engineering, Kyoto Univ., Kyoto 606-8501, Japan

e-mail address : nagaoka@nifs.ac.jp

Abstract. The peaked ion-temperature profile with steep gradient so called ion internal transport barrier (ion ITB) was formed in the neutral beam heated plasmas on the Large Helical Device (LHD) and the high-ion-temperature regime of helical plasmas has been significantly extended. The ion thermal diffusivity in the ion ITB plasma decreases down to the neoclassical transport level. The heavy ion beam probe (HIBP) observed the smooth potential profile with negative radial electric field (ion root) in the core region where the ion thermal diffusivity decreases significantly. The large toroidal rotation was also observed in the ion ITB core and the transport of toroidal momentum was analyzed qualitatively. The decrease of momentum diffusivity with ion temperature increase was observed in the ion ITB core. The toroidal rotation driven by ion temperature gradient so called intrinsic rotation is also identified.

1. Introduction

Improved confinement is a key issue for thermonuclear fusion experiment in stellarator/heliotron devices as well as tokamaks. Internal improved modes have been realized in stellarator/heliotron plasmas using center-focused intense electron cyclotron heating (ECH), for example, electron internal transport barrier (ITB) in the Compact Helical System (CHS) [1], Wendelstein7-AS [2], TJ-II [3] and the Large Helical Device (LHD) [4-6], and the core electron temperature is significantly enhanced by the formation of these electron ITBs. The transition of radial electric field from negative to positive was observed in the formation of electron ITBs and the bifurcation of neoclassical electric field is considered as a mechanism of transition to electron ITB in stellarator/heliotron plasmas [7]. Thus this type of electron ITB is also called as Core Electron-Root Confinement (CERC) [8].

On the other hands, there seems to be large varieties of improved modes in ion transport in stellarator/heliotron such as Heliotron-E [9-10], Wendelstein7-AS [11], CHS [12-13] and LHD [6,14-21]. The role of radial electric field is also considered to be important to understand the improvement of ion transport. The strongly negative electric field at the edge region was observed in the Wendelstein7-AS high density discharges ($n_e=5 \times 10^{19} \text{m}^{-3}$) and a transport barrier was formed there. The behavior of radial electric field can be explained by neoclassical theory [11]. In CHS, two type of improved confinement of ion transport were observed. One is a high- T_i mode in neutral beam heated plasmas with electron density of $1-3 \times 10^{19} \text{m}^{-3}$. The high- T_i mode is realized with low recycling wall condition and characterized by a peaked density profile, a high- T_i (up to 1keV), reduction of ion thermal diffusivity without a reduction of electron thermal diffusivity and an enhanced negative electric field [12]. The other is obtained in electron ITB discharges with low density ($n_e < 0.4 \times 10^{19} \text{m}^{-3}$). The radial electric field is positive in the core and negative at the edge and is consistent with prediction of neoclassical theory. The transport barriers are located at different radial position between electron ($r/a=0.3-0.4$) and ion transport barriers ($r/a \sim 0.6$). It is suggested that the electron transport barrier locates internal region where the positive radial electric field is large

and the ion transport barrier does at the outer region where the shear of radial electric field is large [13].

In tokamak devices, strong and weak ITBs formed depending on the magnetic field configuration and have been studied intensively [22]. The location of strong ITB is related to the position where the safety factor (q) becomes the minimum. The flow shear/radial electric shear was observed at the strong ITB and the shear rate exceeded the turbulence decorrelation rate. The large toroidal rotation in the counter direction was observed at the barrier position in the strong ITB discharges in JT-60U [23], which is considered as a pressure driven toroidal rotation [24]. Recently, toroidal rotation attracts much attention because of suppression of MHD instabilities such as resistive wall mode as well as the link to the radial electric field. Thus, understanding of intrinsic rotation and momentum transport is also a key issue to control the transport and MHD stabilities.

In LHD, a high- T_i plasma characterized by the peaked ion-temperature profile with steep ion temperature gradient, so-called ion ITB, was observed in neutral beam heated plasmas and extended the high- T_i regime of helical plasmas. The large toroidal rotation in the co-direction was also observed in the ion ITB core. In this paper, the reduction of thermal diffusivity of ion ITB plasma and the radial electric field observed by heavy ion beam probe (HIBP) are discussed. The momentum transport and the intrinsic rotation driven by ion temperature gradient are also discussed.

2. Apparatus

The experimental stage is the LHD which is the world's largest superconducting magnetic confinement device employing a heliotron concept [25]. The magnetic field of up to 3 T is provided steadily. The toroidal and poloidal periods are $n = 10$ and $m = 2$, respectively. The major and averaged minor radii are 3.9 m and 0.6 m, respectively. The current plasma heating capability is 21 MW of neutral beam injection (NBI), 2.9 MW of ion cyclotron range of frequency (ICRF) and 2.1 MW of ECH. Three negative-ion-based NBIs (N-NBIs) produce hydrogen neutral beams with the beam energy of 180 keV and total port-through power of 16 MW [26]. The N-NBIs are tangentially injected to LHD plasma (BL1:co, BL2:counter and BL3:co-direction), and the NB driven plasma current and the toroidal momentum input are provided for various types of plasma experiments by means of the combination of N-NBIs. The positive-ion-based NBI (P-NBI) with low energy of 40 keV was perpendicularly injected with the port-through power of 6 MW for high power ion heating experiments [18,27]. In present experiment, ion temperature and rotation profiles are measured by charge exchange spectroscopy (CXs) system [28], and electric field can be observed by CXs only in periphery because of extremely hollowed impurity profile in ion ITB discharges [29]. In the core region, electrostatic potential profile/electric field is measured by heavy ion beam probe (HIBP) [30].

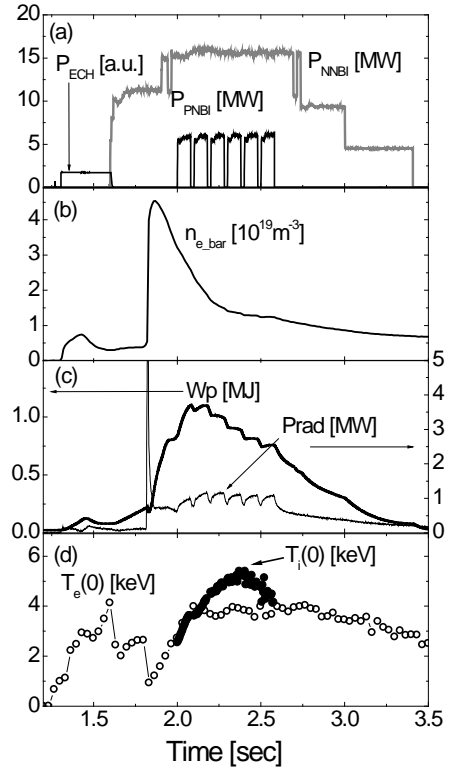


Figure 1. (a) Time evolution of heating power of ECH, N-NBI and P-NBI, (b) average electron density, (c) stored energy and radiation power and (d) central electron and ion temperature.

3. Experimental Results and Discussions

3.1. Ion ITB Discharge

The improvement of ion transport in the core region has been observed and high- T_i plasma beyond $T_i(0) = 5$ keV was realized in NBI heated LHD plasmas [17-18]. Figure 1 shows the typical wave form of high ion temperature plasma with the inwardly-shifted configurations with $R_{ax} = 3.60$ m. The magnetic axis position is an important parameter in LHD experiment because the inward shifted configuration has a good particle confinement and the outward shifted has a good MHD stability in LHD configuration. The magnetic field strength is $B_t = -2.90$ T, and the sign of B_t indicates the direction of coil current; negative value means that the equivalent current is counterclockwise (CCW) corresponding to the co-NBI dominant condition.

A carbon pellet was injected to two N-NBIs sustained plasma at $t = 1.8$ sec then the line averaged electron density rapidly increased. The ion ITB was also observed without carbon pellet injection [17,31] and the achieved ion temperature with carbon pellet is higher than that without carbon pellet. In the density decay phase after carbon pellet injection, the third N-NBI and P-NBI were added to heat plasma with total high power beyond 20 MW of port-through power of NBIs. The ion and electron temperatures increase with decrease of electron density. The central electron temperature saturated at $T_e(0) \sim 4$ keV. Further increase of ion temperature and formation of peaked profile with steep gradient of ion temperature (ion ITB) were observed after saturation of electron temperature, which is shown in Fig. 1-(d). The electron temperature has a broad profile as shown in Fig. 2-(a) and no ITB was observed in electron temperature simultaneously, whereas the profile of ion temperature becomes peaked (ion ITB formation), which is shown in Fig. 2-(b). Then the central ion temperature of $T_i(0) = 5.6$ keV was achieved with the electron density of $n_{e0} = 1.6 \times 10^{19} \text{ m}^{-3}$ (line averaged of $n_e = 1.3 \times 10^{19} \text{ m}^{-3}$). The peaked profile of toroidal rotation in the co-direction was also observed as seen in Fig. 2-(c).

3.2. Reduction of Ion Thermal Diffusivity

Figure 3 shows the ion thermal diffusivity estimated at L-mode phase ($t = 2.01$ sec), transition phase ($t = 2.16$ sec), and ITB phase ($t = 2.36$ sec). The evolution of density and temperature profiles was taken in account. In L-mode phase, the ion thermal diffusivity

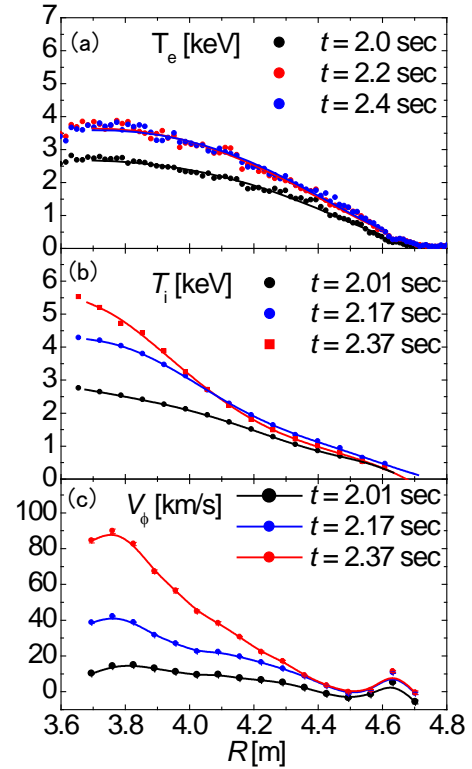


Figure 2. (a) Radial profile of electron temperature measured by Thomson scattering, (b) ion temperature and (c) toroidal flow velocity measured by CXS.

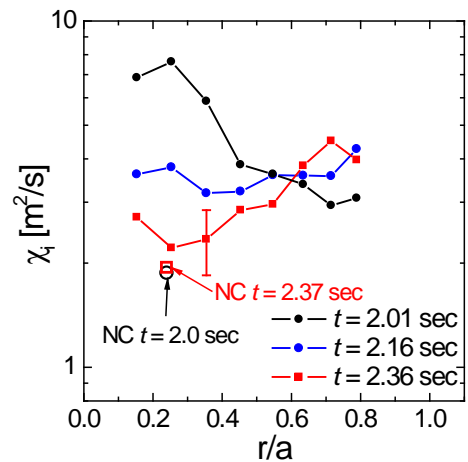


Figure 3. Ion thermal diffusivity as a function of normalized minor radius.

becomes large in the core where ion temperature is high and is roughly scaled by gyro-Bohm scaling; $\chi_i \sim T_i^{1.5}$. After the superposition of additional NBI, the ion thermal diffusivity decreases in time, that is, with increase of ion temperature. The reduction of ion thermal diffusivity with a factor of three was identified in the core region of the ion ITB plasma. The neoclassical transport was calculated by GSRAKE code [32]. In the core region, the neoclassical ion thermal diffusivity is almost unchanged between before and after the transition to the ion ITB, which is also shown in Fig. 3. The neoclassical diffusivity becomes relatively large at the half radius region, because the radial electric field estimated by the neoclassical ambipolarity approaches 0. In the periphery, multiple-roots are predicted by the neoclassical theory. The experimentally obtained ion thermal diffusivity in the ion ITB core reached the same level to the neoclassical one, indicating that the anomalous transport is significantly reduced.

3.3. Radial Electric Field

The radial profile of electrostatic potential was measured by HIBP and CXS in the condition of ctr-NBI dominant condition, because HIBP system works only in the positive B_t (the equivalent current is in CW) conditions. Figure 4-(a) shows the electrostatic potential profile of ion ITB plasma measured by HIBP in the magnetic configuration of $B_t = 2.75$ T and $R_{ax} = 3.60$ m. The ion temperature profile of this plasma is inserted in Fig. 4-(a) and shows clear ion ITB formation. The radial electric field estimated by observed potential profile is shown in Fig. 4-(b) and is negative in the ion ITB region. The neoclassical radial electric field estimated by neoclassical ambipolarity is negative (ion root) in the whole radial position and seems to be consistent with the HIBP observation in the core. In the edge region, the radial electric field was observed by CXS and is positive. The neoclassical positive electric field (electron root) in the edge region marginally disappears in the this discharge. The positive electrostatic potential in the core region is consistent with the positive electric field in the edge region. It is noted that the reduction of anomalous transport in the ion ITB core is realized where the electric field is negative (neoclassical ion root).

Significant outward convection of impurities and resultant extremely hollowed profile of impurities, so-called “impurity hole” were observed in ion ITB plasma [29,33]. The neoclassical transport of impurities is dominated by radial electric field effect and is inward in ion ITB plasmas [34]. It is noted that the compatibility between good confinement of bulk ion and selective exhaust of impurities is an inevitable property for steady state fusion burning plasma operation, and it has been only observed in helical plasmas. The observation of impurity transport characteristics in ion ITB plasma is discussed in another paper in this conference [35].

3.4. Momentum Transport without Intrinsic Rotation

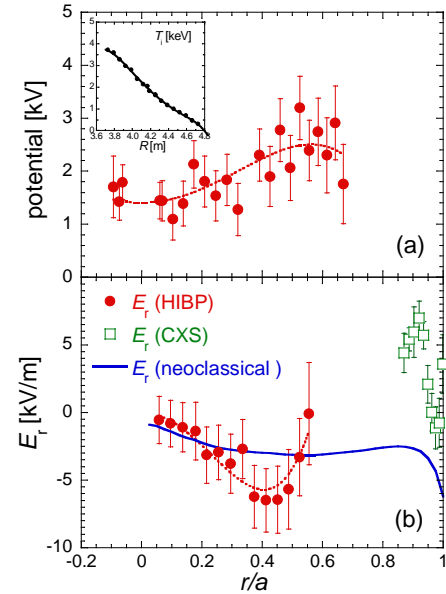


Figure 4. (a) Electrostatic potential profile measured by HIBP and ion temperature profile is also shown in inserted graph. (b) Radial electric field measured by HIBP (closed circles) and by CXS (open rectangles). The solid line indicates the neoclassical electric field.

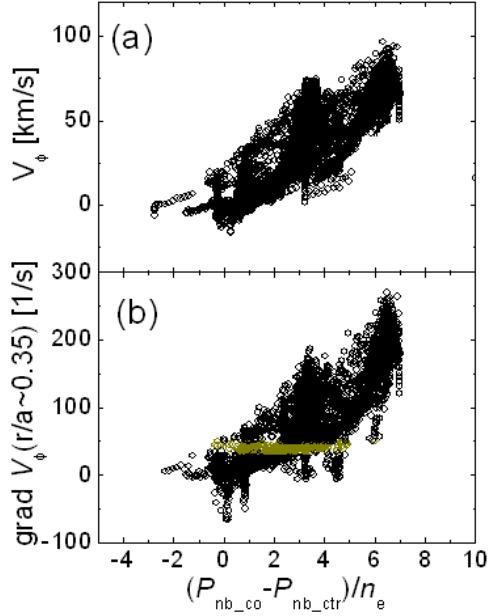


Figure 5. (a) toroidal rotation velocity as a function of torque input normalized by electron density. (b) Gradient of toroidal rotation velocity at a minor radius of $r/a \sim 0.35$. The yellow circles indicate a data set with constant velocity gradient.

As seen in Fig. 2-(c), the peaked profile of toroidal rotation was observed in the ion ITB core region. The direction of toroidal rotation is determined by the momentum input via tangential NBI. The toroidal rotation velocity and the velocity gradient increase with the normalized NBI torque, which is shown in Fig. 5. The gradient of toroidal velocity also increases with ion temperature gradient [36]. These experimental observations suggest the improvement of momentum transport occurs when the ion heat transport is improved. Here we discuss the quantitative estimation of the momentum diffusivity (viscosity).

The quantitative evaluation of local momentum input is required to estimate local momentum transport. The NBI heating profile can be calculated by FIT code for transport study of LHD plasmas. The FIT code was improved, and the momentum depositions profile to electron and ions were also calculated individually. The momentum deposited into electron transfers to ions due to the collision effect, thus the ions eventually receive all momentum deposited by the NBI. In the case of helical plasma, a parallel viscosity is important, because the dumping of toroidal rotation due to the parallel viscosity is significant in the peripheral region. The local momentum flux is written by

$$\Gamma_M = \frac{1}{r} \int \left(T_{\text{ext}} - \frac{\partial m_i n_i V_t}{\partial t} - \mu_{\parallel} m_i n_i V_t \right) r dr, \quad (1)$$

where Γ_M , T_{ext} , m_i and μ_{\parallel} are the radially transported momentum flux, external momentum input calculated by FIT code, ion mass and parallel viscosity, respectively. The second term indicates the effect of profile changes in time. The third term indicates the damping of the toroidal rotation due to magnetic field ripple. The parallel viscosity is calculated by

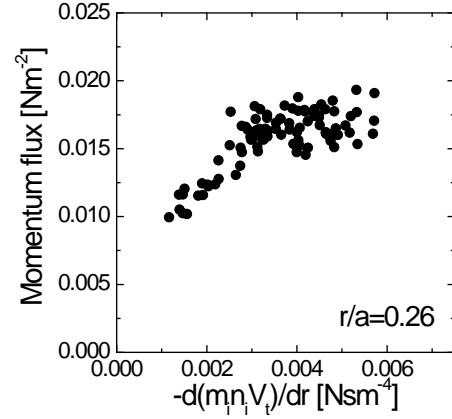


Figure 6. Radial flux of toroidal momentum as a function of momentum gradient at the radial position of $r/a = 0.26$.

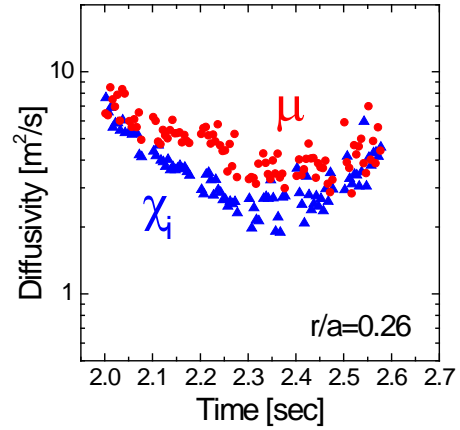


Figure 7. Time evolution of ion thermal diffusivity (χ_i) and viscosity (μ) at the radial position of $r/a = 0.26$.

neoclassical theory and is negligibly small in the plasma center and large at the periphery. The flux and gradient relation of momentum transport is shown in Fig. 6. In the L-mode phase, the gradient of toroidal momentum increases with the radial momentum flux, whereas it increases with an almost constant momentum flux in the ion ITB phase. The heat and momentum diffusivities are compared in Fig. 7, in which the off-diagonal terms such as intrinsic rotation are not taken in account. The ion thermal diffusivity decreases in the transition phase from L-mode to ion ITB phase and the viscosity behaves similarly, thus the momentum transport is also improved in the ion ITB plasma. The absolute value of viscosity is same order with the ion thermal diffusivity, that is, Prandtl number($=\mu/\chi_i$) is 0.5-1.0.

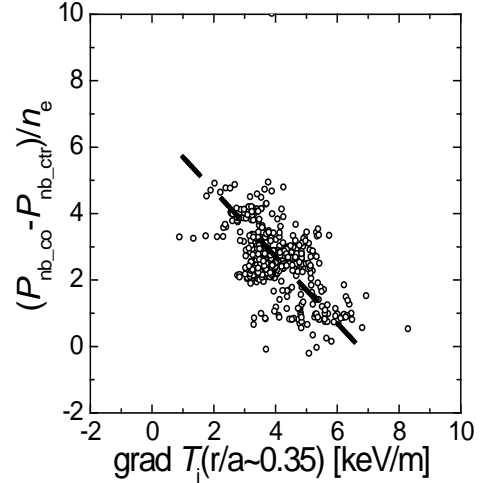


Figure 8. Normalized input torque corresponding to momentum flux as a function of ion temperature gradient at the minor radius of $r/a = 0.35$.

3.5. Effect of Intrinsic Rotation Driven by Ion Temperature Gradient

Here other effects on momentum transport are discussed. The radial momentum flux is considered to be given by the radial gradient of plasma parameters such as temperature, electrostatic potential, density and so on,

$$\Gamma_M = f(\nabla V_t, \nabla T_i, \nabla \phi, \dots), \quad (2)$$

where f and ϕ are a function and electrostatic potential, respectively. The velocity gradient dependence is a diagonal term corresponding to viscosity. The temperature and potential gradient effects are off-diagonal effects, or so-called intrinsic rotation. The flux-gradient relation of toroidal rotation (Fig. 6) shows an offset of momentum transport, indicating an existence of off-diagonal effect. The potential gradient (electric field) in ion ITB core is weakly negative and almost constant during discharge. In order to investigate the temperature gradient effect, the data set with a constant velocity gradient shown in Fig. 5-(b) with colored circles is plotted in Fig. 8 as a function of temperature gradient. The external torque normalized by density (the vertical axis of Fig. 8) is directly related to the momentum flux given by eq. (1), in which the velocity gradient and parallel viscosity are almost constant in present condition. Thus, the existence of temperature gradient effect on the momentum transport was identified in the ion ITB plasmas. The dependence shown in Fig. 8 means an intrinsic rotation in the co-direction driven by ion temperature gradient. This observation is consistent with previous observation of intrinsic rotation without ion ITB discharges [37]. The qualitative evaluation of off-diagonal terms and diagonal term are required for further understanding of transport linkage among particles, momentum and heat, which is left for the future study.

4. Summary

The ion ITB formed in NBI heated plasmas of LHD and is characterized by peaked temperature and toroidal rotation profiles with steep gradient, power threshold, no ITB in electron temperature profiles. The ion temperature of 5.6 keV was achieved with a carbon pellet injection discharge. The ion thermal diffusivity decreases with a factor of three was identified in the ion ITB core and reaches the neoclassical transport level. The radial electric field in the ion ITB core region was observed by HIBP and is negative (ion root), which is

consistent with theoretical prediction based on neoclassical ambipolarity. The large rotation velocity was observed in the ion ITB core and the momentum transport is also improved there. The intrinsic rotation in the co-direction driven by temperature gradient was identified in the core region.

Acknowledgements

One of the authors (K.N.) would like to thank Profs. K Itoh (NIFS), S-I. Itoh (Kyushu Univ.), A. Fujisawa (Kyushu Univ.), Dr. Y. Kamada (JAEA) for fruitful discussions and the technical staff in LHD project for their support of these experiments. This work is partially supported by National Institute for Fusion Science (NIFS-ULBB501, NIFS-ULBB510) and a Grant-in-aid for Scientific Research (18206094).

References

- [1] A. FUJISAWA et al., "Electron Thermal Transport Barrier and Density Fluctuation Reduction in a Toroidal Helical Plasma", *Phys. Rev. Lett.* **82**, 2669 (1999).
- [2] H. MAASSBERG et al., "The neoclassical "Electron Root" feature in the Wendelstein-7-AS stellarator", *Phys. Plasmas* **7**, 295 (2000).
- [3] F. CASTEJON et al., "Enhanced heat confinement in the flexible heliac TJ-II", *Nuclear Fusion* **42**, 271 (2002).
- [4] T. SHIMOZUMA et al., "Formation of electron internal transport barriers by highly localized electron cyclotron resonance heating in the large helical device", *Plasma Phys. Controlled Fusion*, **45**, 1183 (2003).
- [5] K. IDA et al., "Characteristics of electron heat transport of plasma with an electron internal-transport barrier in the Large Helical Device", *Phys. Rev. Lett.* **91**, 085003 (2003).
- [6] Y. TAKEIRI et al., "Formation of electron internal transport barrier and achievement of high ion temperature in Large Helical Device", *Phys. Plasmas*, **10**, 1788 (2003).
- [7] A. Fujisawa, "Internal Transport Barrier and Bifurcation Phenomena in Stellarators", *Fusion Science and Technology*, **46**, 91, (2004).
- [8] M. Yokoyama et al., "Core electron-root confinement (CERC) in helical plasmas", *Nuclear Fusion*, **47**, 1213, (2007).
- [9] K. IDA et al., "High ion temperature mode in Heliotron E", *Phys. Rev. Lett.* **76**, 1268 (1996).
- [10] F. SANO et al., "Ion and electron energy balance calculations for neutral-beam-heated Heliotron-E plasmas", *Nucl. Fusion*, **24**, 1103 (1984).
- [11] M. KICK et al., "High ion temperatures and high beta in W7-AS" Proc. 16th IAEA Conf. on Fusion Energy (Montreal, 1996) vol.2 (Vienna:IAEA) p.17.
- [12] K. IDA et al., "Transition from L mode to high ion temperature mode in CHS heliotron/torsatron plasmas", *Nuclear Fusion* **39**, 1649 (1999).
- [13] T. MINAMI et al., "Increased understanding of neoclassical internal transport barriers in CHS", *Nuclear Fusion* **44**, 342 (2004).
- [14] Y. TAKEIRI et al., "High-ion temperature experiments with negative-ion-based neutral beam injection heating in Large Helical Device", *Nucl. Fusion*, **45**, 565, (2005).
- [15] S. MORITA et al., "Recent Progress on Confinement Improvement Study and Ion Heating Experiments in LHD", *Problems of Atomic Science and Technology*, **10**, 3 (2005).
- [16] Y. TAKEIRI et al., "Confinement improvement in high-ion temperature plasmas heated with high-energy negative-ion-based neutral beam injection in the Large Helical Device", *Nucl. Fusion*, **47**, 1078 (2007).

- [17] M. YOKOYAMA et al., “Extension of High-Ion-Temperature Regime in the Large Helical Device (LHD)”, *Phys. Plasmas*, **15**, 056111-1 (2008).
- [18] K. NAGAOKA et al., “Ion Heating Experiments Using Perpendicular Neutral Beam Injection in the Large Helical Device”, *Plasma Fusion Res.*, **3**, S1013-1 (2008).
- [19] S. MORITA et al., “Increase of Central Ion Temperature after Carbon Pellet Injection in Ne-Seeded NBI Discharges of LHD”, *J. Plasma Fusion Res.*, **79**, 641 (2003).
- [20] S. MORITA et al., “Behavior of ion temperature in electron and ion heating regimes observed with ECH, NBI and ICRF discharges of LHD”, *Nucl. Fusion*, **42**, 1179 (2002).
- [21] K. Nagaoka et al., “ION HEATING EXPERIMENTS AND IMPROVEMENT OF ION HEAT TRANSPORT IN LHD”, *Fusion Science and Technology*, **58**, 46, (2010).
- [22] R C Wolf, “Internal transport barriers in tokamak plasmas”, *Plasma Phys. Control. Fusion*, **45**, R1, (2003).
- [23] Y. Sakamoto, et al., “Characteristics of internal transport barriers in JT-60U reversed shear plasmas”, *Nucl. Fusion*, **41**, 865, (2001).
- [24] M. Yoshida, et al., “Role of Pressure Gradient on Intrinsic Toroidal Rotation in Tokamak Plasmas”, *Phys. Rev. Lett.*, **100**, 105002, (2008).
- [25] A. IYOSHI et al., “Overview of the Large Helical Device project”, *Nuclear Fusion* **39**, 1245 (1999).
- [26] Y. Takeiri, et al., “High Performance of Neutral Beam Injectors for Extension of LHD Operational Regime”, *Fusion Sci. Tech.*, **58**, 482, (2010).
- [27] M. Osakabe, et al., “Development of Radial Neutral Beam Injection System on LHD”, Proc. 17th Int. Toki Conf./16th Int. Stellarator/Heliotron Workshop 2007, Toki, P2-079, (2007).
- [28] M. Yoshinuma, et al., “Chage-Exchange Spectroscopy with Pitch-Controlled Double-Slit Fiber Bundle on LHD”, *Fusion Sci. Tech.*, **58**, 375, (2010).
- [29] M. Yoshinuma et al., “Observation of an impurity hole in the Large Helical Device”, *Nuclear Fusion*, **49**, 062002-1, (2009).
- [30] T. Ido, et al., “Development of 6-MeV Heavy Ion Beam Probe on LHD”, *Fusion Sci. Tech.*, **58**, 436, (2010).
- [31] K. Ida et al., Ion internal transport barrier in Large Helical Device, *Contributions to Plasma Physics*, **50**, 558, (2010).
- [32] C D Beidler and W D D’haeseleer, “A general solution of the ripple-averaged kinetic equation (GSRAKE)”, *Plasma Phys. Control. Fusion*, **37**, 463, (1995).
- [33] K. Ida et al., “Observation of an impurity hole in a plasma with an ion internal transport barrier in the Large Helical Device”, *Physics of Plasmas*, **16**, 5, 056111, (2009).
- [34] T. Ido, et al., Invited talk in 37th EPS conference on Plasma physics, 21-25 June, 2010, Dublin, Ireland.
- [35] M. Yoshinuma, et al., presented in 22nd IAEA-FEC, 11-16 Oct, 2010, Daejeon, Korea (this conference).
- [36] K. Ida et al., “Spontaneous Toroidal Rotation Driven by the Off-diagonal Term of Momentum and Heat Transport in the Plasma with Ion Internal Transport Barrier in LHD”, *Nuclear Fusion*, **50**, 064007-1, (2010).
- [37] M. Yoshinuma et al., Observations of spontaneous toroidal flow in the LHD, *Nuclear Fusion*, **49**, 075036, (2009).